Int J Adv Manuf Technol (2017) 92:2185–2195
DOI 10.1007/s00170-017-0293-2

ORIGINAL ARTICLE

Effect of external longitudinal magnetic field on arc plasma characteristics and droplet transfer during laser-MIG hybrid welding

Xun Zhang[1] · Zeyang Zhao[1] · Gaoyang Mi[1] · Chunming Wang[1] · Ruoyang Li[1] · Xiyuan Hu[1]

Received: 3 September 2016 / Accepted: 13 March 2017 / Published online: 30 March 2017

Abstract The arc plasma behavior and droplet transfer are investigated using laser-MIG (metal insert gas) hybrid welding assisted by an external longitudinal magnetic field. The characteristic of arc plasma and droplet transfer can be recorded via combining sensing of the welding current and arc voltage with a high-speed imaging. Results indicated that the external longitudinal magnetic field had a significant impact on the arc shape, droplet formation, droplet size, and detaching. Under the magnetic field, the arc shape became a triangle gradually, and the off-axis arc and droplet gradually pointed to the axis of the filler wire. In addition, it has been found that with increasing the magnetic induction intensity, the droplet diameter and cycle time can be reduced. The mechanism of these phenomena was also further analyzed.

Keywords Magnetic field · Laser-MIG hybrid welding · Arc plasma characteristic · Droplet transfer

1 Introduction

In recent years, laser-arc hybrid welding technology has received a significant attention, because of its many advantages, including deeper welding penetration, the ability to bridge relatively large gaps, a higher welding speed, and so on [1]. Laser-MIG hybrid welding is one of the most promising processes in the development of a high-efficient and high-quality manufacturing because it overcomes the individual drawbacks associated with the MIG and laser welding.

So far, many researches on laser-arc hybrid welding have been done to study the arc characteristic. The most important phenomenon of the arc characteristic is the interaction and coupling effect between the laser-induced plasma and arc. It is well-known that the laser compresses the arc and attracts the arc. The current, laser power, and the distance between the laser and arc (D_{LA}) are the most three important parameters, influencing the interaction of the arc and laser-induced plasma [2, 3]. Wang et al. [4] showed that the hybrid plasma formed a curved channel between the welding wire and keyhole. Gao et al. [5] discovered that the efficient synergetic effect between the laser and arc can be only obtained with suitable shielding gas parameters. And for the mechanism of the phenomenon [6], the most commonly accepted explanation is that laser-induced plasma produces ionized plasma and this ionized plasma has a number of charged particles to form a current path which offers less resistance than the arc. Because of the principle of minimum voltage, the welding current tends to pass through the path with the least resistance and a low voltage.

In general, there are three major droplet transfer modes including short-circuiting, globular, and spray. The factors that affect the droplet transfer mode are the hybrid welding current, D_{LA}, laser power, and shielding gas. Campana et al. [7] indicated that the optimal D_{LA} for laser-MIG hybrid welding was 2–3 mm in order to avoid turbulence in the weld pool and disturbance of the keyhole formation and achieve synergy between the processes. Tani et al. [8] reported that a 30 up to 40% helium content gas can stabilize the droplet transfer and form a good appearance. Liu et al. [9] found that the arc energy determined the mode of droplet transfer. Zhang et al. [10] proposed that laser-induced plasma significantly affected the forces acted on the droplet that determined the droplet

✉ Chunming Wang
hust_wangcm@163.com; cmwang@mail.hust.edu.cn

[1] School of Materials Science and Engineering, Huazhong University of Science and Technology, Wuhan 430074, People's Republic of China

transfer mode, and the changed electromagnetic force that increased droplet size and droplet formation time. Liu et al. [11] and Gao et al. [12] found that the droplet transfer mode related to arc power and laser power affects the behavior of droplet transfer in laser-MAG (metal active gas) and MIG hybrid welding. Guen et al. [13] observed that the short-circuiting transfer occurred between 100 and 200A, the globular mode between 200 and 250A and the spray mode from 250 to 400A in the YAG laser-MAG arc welding processes.

The study on application of the longitudinal magnetic field to arc welding started early. As early as 1970s, Blinkov et al. [14] started to investigate the interaction between the longitudinal magnetic field and TIG (tungsten electrode insert gas) arc. In recent years, it is widely investigated, including the application to TIG welding, MIG welding, short-circuit MAG welding, swiveling-jet MAG welding, submerged-arc welding, and cold metal transfer welding [15–19]. The common discoveries were that the arc rotated at a high speed, the shape became a bell-type, and arc-upside shrank while arc-bottom expanded. Furthermore, Hartz-Behrend et al. [20] indicated that the magnetic field reduced the energy load, the molten metal, and the thermal stress of the workpiece during arc welding. Chang et al. [21] analyzed the impact of the external longitudinal magnetic field on droplet transfer during short-circuit MIG welding, and found the resultant force in the z direction and horizontal direction could be increased by low-frequency magnetic fields (5–25 Hz), and these positive impacts could promote the metal transfer and reduce the spatter.

Furthermore, except for the investigation of arc welding assisted by magnetic field, applying the magnetic field into the laser welding is also widely studied. Zhou and Tsai [22] pointed out that the reinforcement, cross-sectional shape, and the top surface of the weld bead can be changed by applied an external magnetic field. Liu et al. [23] suggested that the magnetic field can increase the penetration of the laser welding by reducing the density of the plasma. And the magnetic stirring by applying the magnetic field has a significant influence on the dilution of the weld bead in laser welding, indicating that the magnetic field can reduce the welding defects, like hot cracks and porosity [24, 25]. Bechmann et al. [26] simulated the influence of a transversal magnetic field on weld shape combined with experimental work in high-power laser welding of thick aluminium parts. It found that the shape of weld bead changed from a wineglass shape to a V-shape. Yu et al. [27] discovered that the rotated magnetic field can refine the grain in laser welding of Al-Si12 alloy. It was explained that the liquid metal in molten pool rotated because of the Lorentz force, which caused by the induced current of magnetic field cutting the liquid metal. Besides, the magnetic field can be as a support force to improve weld sagging. Experimental and simulative results have shown that a proper magnetic induction intensity can allow the single-pass laser welding without sagging or drop-out of melt [28]. Sun et al. [29] found that the sidewall penetration increased obviously with increased magnetic induction intensity or decreased magnetic field frequency in TIG narrow gap welding.

Considering the discussions above, few researched have been reported on the application of magnetic field to laser-MIG hybrid welding. However, there are some problems in the application of laser-MIG hybrid welding, such as the arc drifting, lack fusion of sidewalls during narrow gap hybrid welding, humps during high-speed hybrid welding, etc. Hence, how to improve the stability of the hybrid welding further is becoming quite important, and the magnetic field is a good way to make it. In this paper, an external longitudinal magnetic field was brought into laser-MIG hybrid welding. In addition, a high-speed camera system was performed to analyze the effect of magnetic field on arc plasma and droplet transfer with the aim of optimizing laser-MIG hybrid welding.

2 Experimental method

2.1 Materials

SUS316L austenitic stainless steel with the dimension of 200 mm × 150 mm × 4 mm was employed in this study. The specimen surface was chemically cleaned by acetone before welding to eliminate surface contamination. Austenitic stainless steel ER316LSi filler wire was also used with 1.2 mm diameter. The chemical compositions (wt%) of base metal and filler wire are given in Table 1.

2.2 Experimental equipment

Bead-on-plate welds were made using a 4 kW fiber laser (IPG YLR-4000). The fiber laser with an emission wavelength of 1.07 μm can deliver in continuous wave (CW) mode. Laser beam was passed through focusing mirror with the focal length of 250 mm and was finally focused as a spot of 0.3 mm in diameter. A Fronius TPS4000 digital inverter arc-welder power was used as the MIG welding power, achieving the integration of regulation of current, voltage, and wire feed rate. So, the

Table 1 The chemical compositions of base metal and filler wire

	C	Mn	Si	S	P	Cr	Ni	Mo	Fe
Base metal	≤0.03	≤2.00	≤0.75	≤0.030	≤0.045	16.0–18.0	10.0–14.0	2.0–3.0	Bal.
Filler wire	≤0.03	1.0–2.5	0.83	≤0.020	≤0.030	18.0–20.0	11.0–14.0	2.5–3.0	Bal.

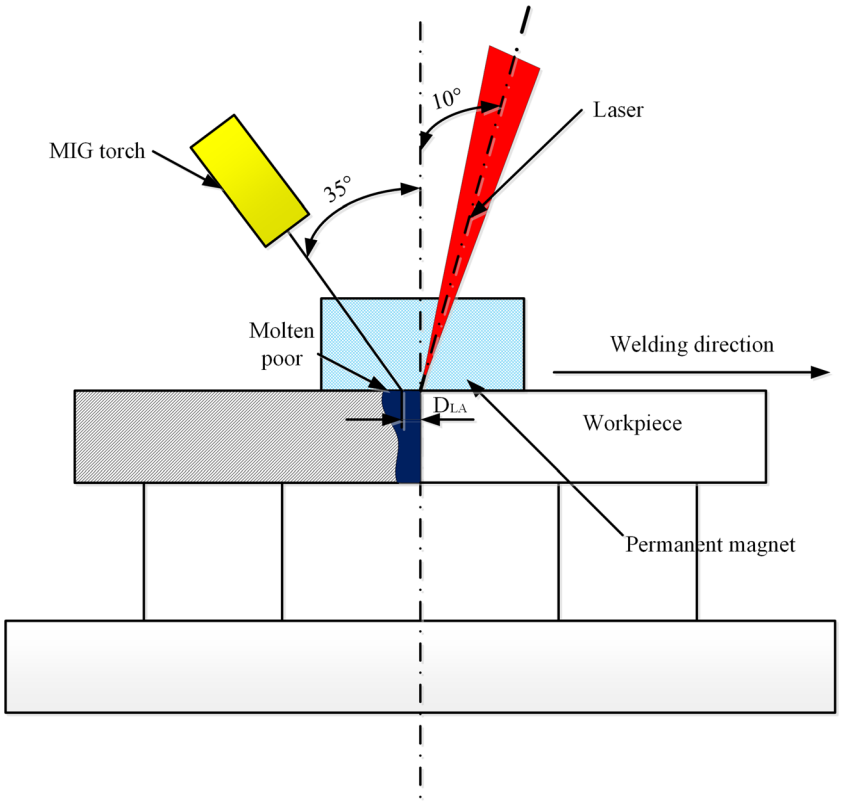

Fig. 1 Schematic of laser-MIG hybrid welding with an external longitudinal magnetic field setup

current was the only parameter to express the arc parameters in this paper. The angle between laser and perpendicular direction was 10°, and the angle between MIG torch and perpendicular direction was 35°. A ferrite permanent magnet with a dimension of 110 mm × 105 mm × 15 mm, which the surface magnetic induction intensity was 120 mT, was used as the source of magnetic field. And the magnetic induction intensity can change by adjusting the distance between the permanent and the base metal. A high-precision gauss meter (HT-201) was used to measure the magnetic induction intensity. The schematic of the setup is shown in Fig. 1.The shielding gases used for arc torch are the pure argon (99.999%Ar), flowing velocity of which was 20 L/min. The welding parameters are provided in Table 2. A CMOS MV-D1024E high-speed camera (Photonfocus, Switzerland) with a recorded speed of 38,000 frames per second was used to capture the welding phenomena, as shown in Fig. 2. In this paper, the sample frequency for arc/plasma was 2267 frames per second and 2686 frames per second for droplet, respectively.

The hybrid welding current was measured by a Hall-effect current sensor (CS300E2, Chieful). The hybrid welding voltage was measured by a Hall-effect voltage sensor (VSM025A, Chieful) at the contact tip. The data acquired by these two sensors was recorded using a high-performance multichannel, digital, and timing I/O board (6211E, NI) to a computer, and processed by LabVIEW.

Table 2 Welding parameters

Welding parameters	
Laser power P (kW)	2.0
MIG current I (A)	150
Welding speed v_m (m/min)	1.1
Angle of MIG torch and laser torch θ(°)	45
Focal point position Δf (mm)	0
Distance between laser and arc D_{LA} (mm)	2
Magnetic induction intensity B (mT)	0, 8, 12, 16, 22

2.3 Measurement of arc characteristics and droplet transfer

As schematically shown in Fig. 3, the arc characteristics of hybrid welding, defined by its root diameter (D_R), bottom

Fig. 2 MV-D1024E high-speed camera

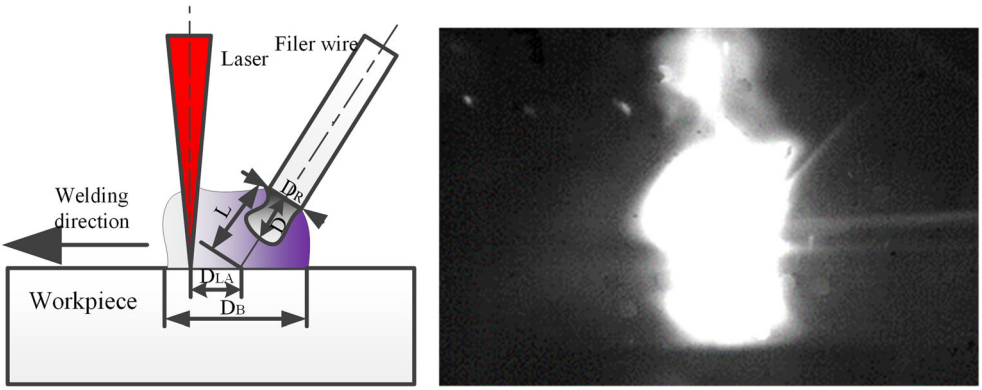

Fig. 3 Schematic of **a** arc and droplet dimensions of hybrid welding and **b** typical arc/plasma of hybrid welding

diameter of arc (D_B), was suitably measured by a properly professional computerized software using these high-speed images. The behavior of droplet transfer was also studied by the measurement of diameter (D) and droplet transfer cycle (T_C).

2.4 Experimental process

The schematic of the experimental setup is shown as Fig. 4. The samples were firmly fixed flat on the jig so that the welding optics were inclined to the direction of the welding and the workpiece surface to prevent splash metal from damaging the lens during the laser welding. And the permanent magnet was fixed under the samples con currently. During this process, the welding speed was set up via controlling the numerical-controlled machine, ensuring that the high-speed camera was alignment to the region of arc/plasma.

3 Results and discussion

3.1 Arc plasma phenomena of hybrid welding assisted by magnetic field

Figure 5 graphically shows the typical arc/plasma phenomena of laser-MIG hybrid welding without magnetic field. From these images, it is obviously that the arc and laser-induced plasma are a whole, and the direction of arc is not parallel with the direction of filler wire but has a deflection to keyhole because of laser-induced plasma attracting. However, the hybrid plasma is unstable, which means the arc cannot be attracted or coupled steadily. As revealed in Fig. 6, when there is a longitudinal magnetic field during the hybrid welding process, the arc/plasma shape and coupling effect change obviously. Compared with Fig. 5, the common transformation of arc with the magnetic field is that the bottom diameter of arc is bigger than that without magnetic field and arc rotates with a high velocity. And with

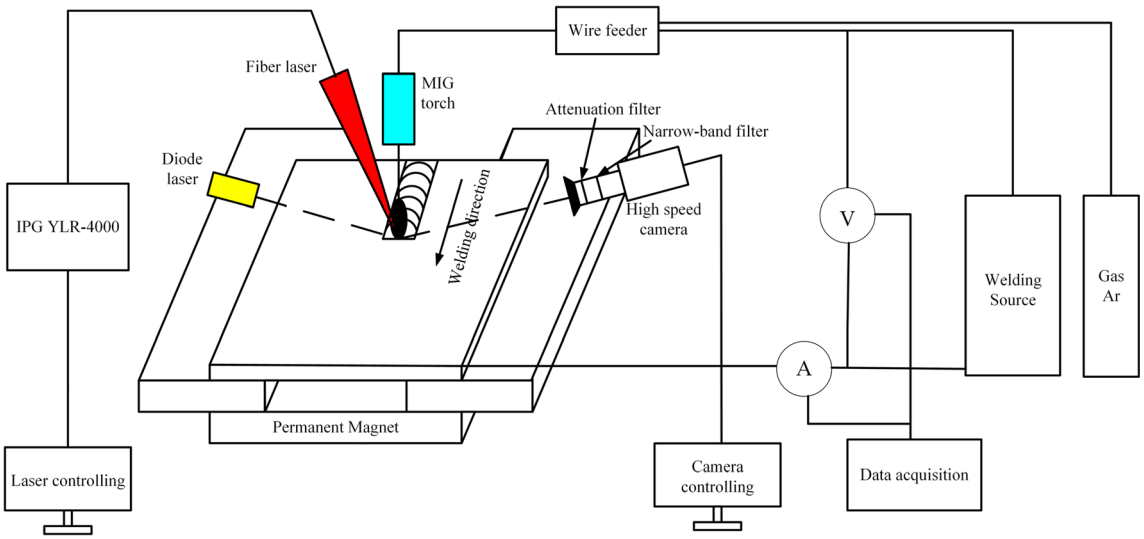

Fig. 4 Schematic of the experimental setup for arc plasma and droplet transfer observation of hybrid welding phenomena

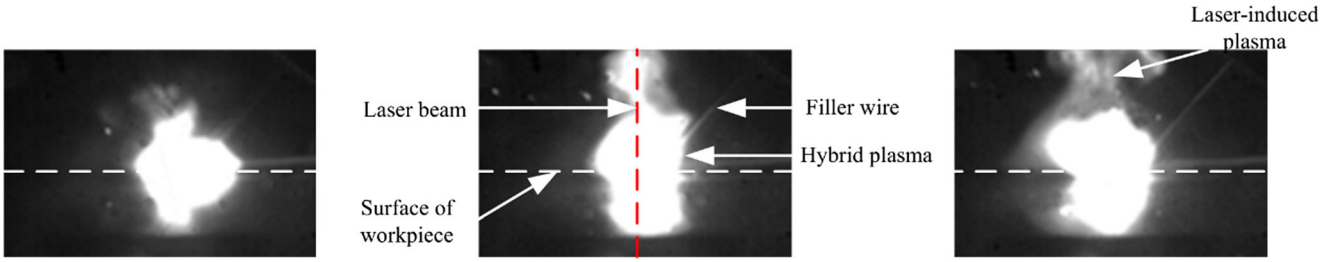

Fig. 5 Typical arc/plasma phenomena of hybrid welding without external longitudinal magnetic field

increasing the magnetic induction intensity (B), the shape of arc becomes triangle gradually. The arc appears a condition, the root shrinks of which and bottom enlarges. The further results, as displayed in Fig. 6a, b, clearly demonstrate that the arc direction is parallel with the filler wire. In addition, Fig. 6c presents the arc points to downward direction of filler wire when B is equal to 16 mT. But with B increasing to 22 mT, shape of arc is unstable by comparison to (a)–(c). From Fig. 6d, it is obviously that arc rotating velocity is too large so that the arc waggles acutely. On the other hand, the laser-induced plasma weakens with increasing B. And the arc is dominant for the coupling of these two heat sources. Considering these results, what happens is that arc rotating with high velocity enhances the arc stiffness, which strengthens the ability to resist in attracting by laser-induced plasma. This rotation leads the arc to a more perpendicular position with increasing B. Moreover, Fig. 6 reveals that an appropriate magnetic field further improves the arc stabilization further in comparison to Fig. 5.

The D_R, D_B which are the average of the measured values of 30 random selected high-speed camera images, offer an easier

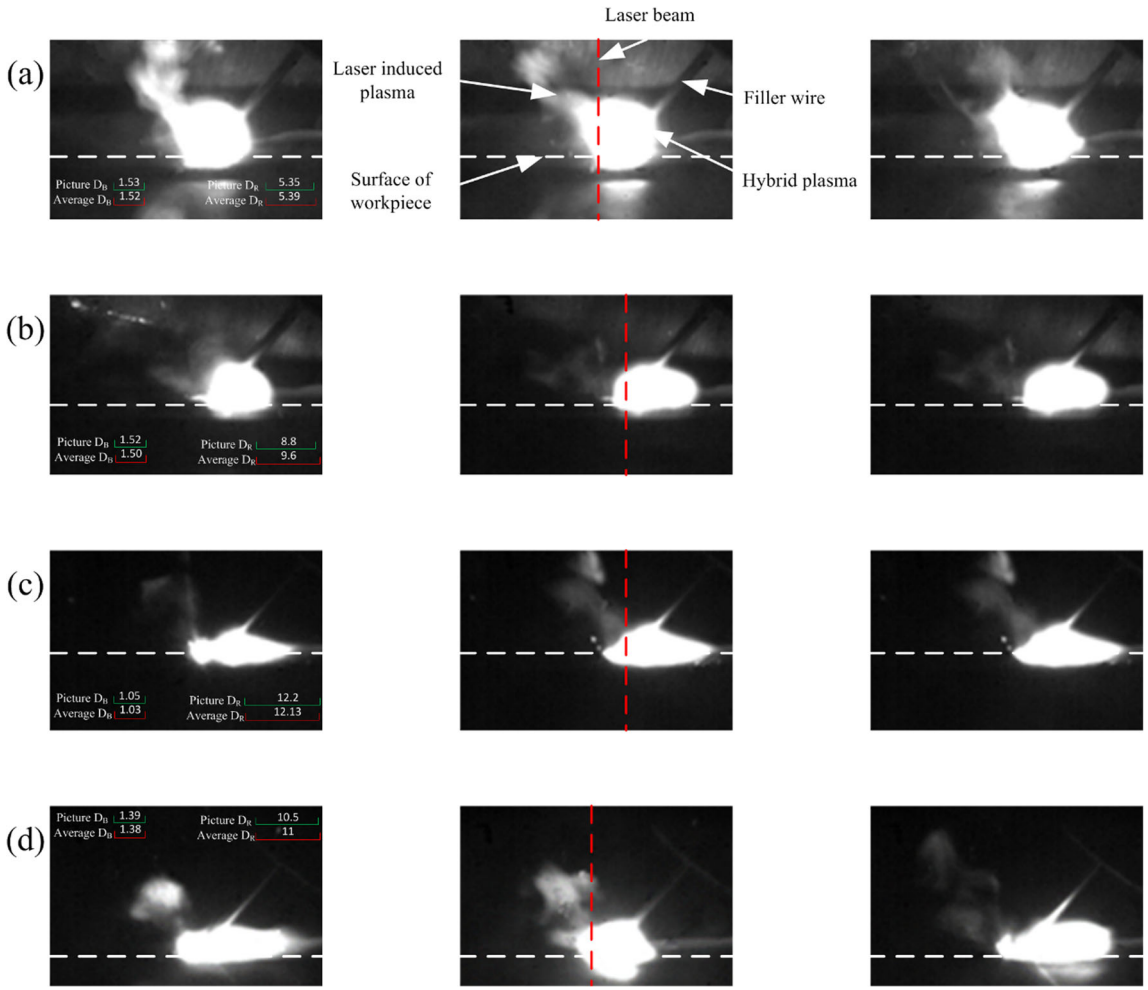

Fig. 6 Typical shape of arc/plasma with different magnetic induction intensity (B) of hybrid welding **a** B = 8mT **b** B = 12mT **c** B = 16mT **d** B = 22mT

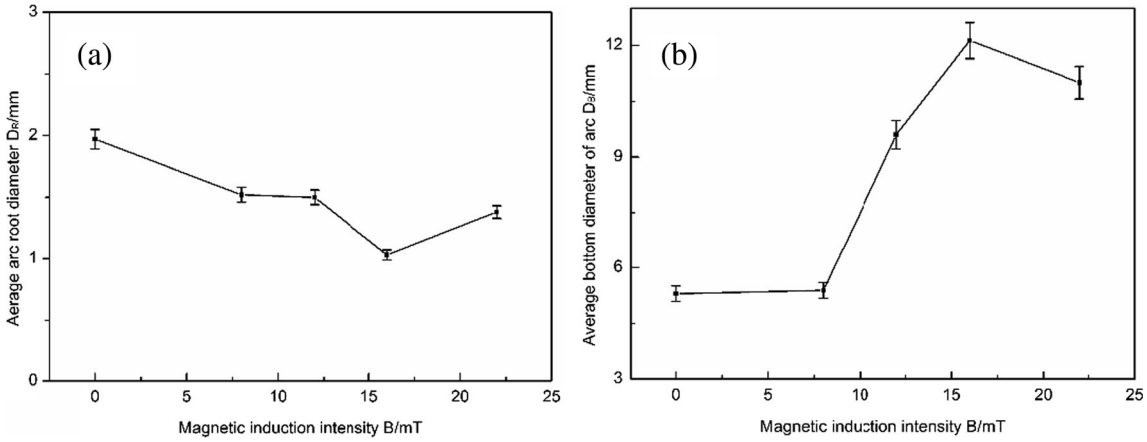

Fig. 7 At different magnetic induction intensity on **a** average arc root diameter **b** average bottom diameter of arc

way to illustrate the change of the arc shape. Figure 7a points out that D_R decreases with B increasing, and D_R is the smallest under this condition of 16 mT. As seen from Fig. 7b, D_B increases a little when B is 8 mT. But with the B increasing to 16 mT, D_B has a quickly raising. Subsequently, D_B falls a little when the B increases to 22 mT.

With applying the magnetic field, the arc and laser-induced plasma shapes are extremely changed. In our previous work [30], it is well revealed that the mechanism of arc changing. The mechanism analysis of arc rotating under longitudinal magnetic field was achieved, so they were not described again here. The arc is a conductor with some flexibility so that it would be influenced. However, under an external longitudinal magnetic field, because the arc rotates at a high speed, the arc flexibility weakens while stiffness is greatly enhanced. As B increasing, the arc stiffness is remarkably enhanced. Consequently, it is strengthened for arc to resist the attracting from the laser-induced plasma. When there is no magnetic field, because of the laser-induced plasma containing a lot of metal ionization, according to the principle of minimum voltage, the arc conducts through the laser-induced plasma, resulting in deviation of arc, as shown in Fig. 8a. If B is small (8 and 12 mT), the arc stiffness is greatly enhanced, so a conductive path directly forms between the filler wire and workpiece as shown in Fig. 8b. And if B is relatively high (16 and 22 mT), the arc stiffness is enhanced further, so as to lead to the axis of the arc apart from laser-induced plasma further. Meanwhile, the impact of laser-induced plasma on arc weakens to almost negligible, as shown in Fig. 8c. Considering these, however, it is not signified that the external magnetic field is not good to laser-arc hybrid welding. Under appropriate magnetic field parameter (12 to 16m T), it is more stable for this process and the coupling is more mightiness.

3.2 Droplet transfer phenomena of hybrid welding assisted by the magnetic field

Figure 9 presents the results of the droplet transfer, welding current, and welding voltage waveforms without external longitudinal magnetic field. These images clearly display the typical feature of the short-circuiting transfer mode during laser-MIG hybrid welding. The globules of molten metal periodically bridges the gap between the tip of the wire and weld pool. When the globule touches the surface of the molten pool, the current rises to a high value rapidly, while the voltage drops to a much lower value and the arc dies out simultaneously. Besides, a liquid bridge is produced under the combination effect of the surface tension and electromagnetic forces. With rapidly increasing welding current, a necking appears at the liquid bridge owing to electromagnetic pinch effect. And then, the droplet implodes at the liquid bridge with fine spatters. As soon as the filler wire disaffiliates from the molten pool, the current and voltage recover to the normal value and the arc burns again [9]. Then the process above

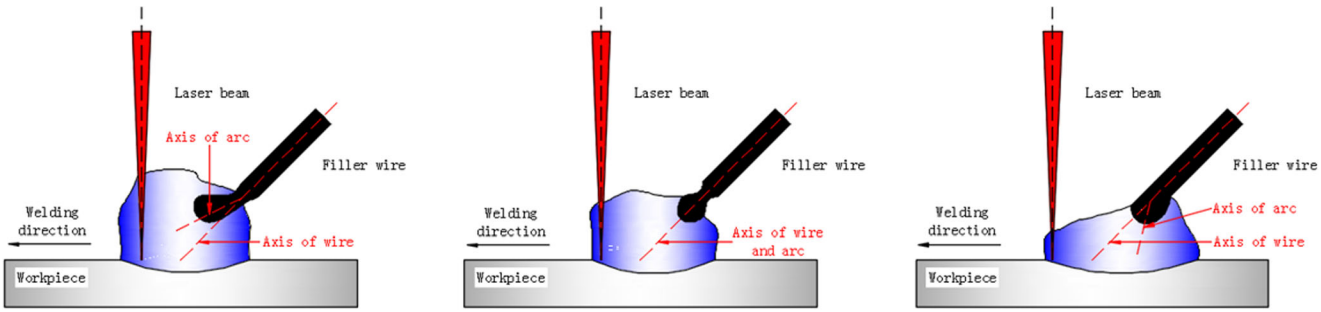

Fig. 8 Magnetic induction intensity influence on plasma trajectory and droplet appearance on laser-MIG hybrid welding. **a** Without magnetic field; **b** with relatively low magnetic induction intensity; **c** with relatively high-magnetic induction intensity

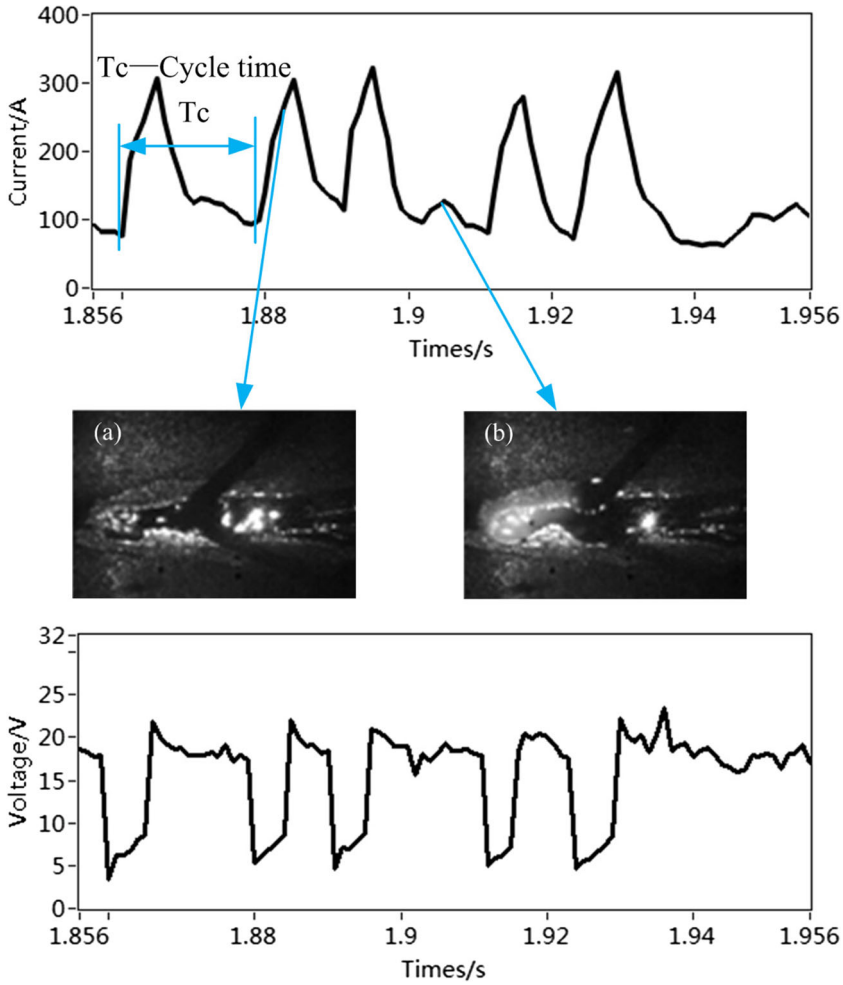

Fig. 9 Droplet transition images, and characteristics of current and voltage during hybrid welding without magnetic field

could be repeated. During this process, the high-speed image, as seen in Fig. 9b, clearly describes that the droplet is deviation from the axis of filler wire. And there are two reasons for this phenomenon: (1) The vapor jet force is a retention force for droplet transfer, and its direction is vertically up. (2) The arc is attracted by the laser-induced plasma which changes the direction of plasma drag force, as shown in Fig. 5. And this force is the main driving force of droplet transfer. Because of the droplet deviation, the droplet may shield the route of laser, or falls into the keyhole nearby, even into the keyhole directly, which affects the coupling effect and makes more spatters.

Hua et al. [31] found that the welding current and voltage became more stable and had less fluctuations with external longitudinal magnetic field during arc welding. Figure 10 exhibits characteristics of current and voltage during laser-MIG hybrid welding. It can be seen that the waveform of the welding current and voltage shifted a great deal. First, when B is 8 mT, the welding peak current has a decrease trend compared without magnetic field. However, it is not outstanding. With B increasing to 12 and 16 mT, as against these two conditions contrast with 0 mT, it is obviously that the peak currents are smaller than $B = 0$ mT. But B increasing to 22 mT, the current amplitude is not stable. This verified the high-speed images in Fig. 6. The peak current represents how easily the droplet transfers when the droplet touches the molten pool. So, it is more easily for droplet transferring on account of the peak current decrease, and it may shorten the transfer cycle time. Secondly, the cycle time of current (T_C) becomes distinctly short and stable when B is 8, 12, and 16 mT. Twenty-two milliteslas of B of T_C is also shorter, but is not stable. Combined with the high-speed camera images in Fig. 6b, it suggests that the arc and hybrid composite plasma are unstable under this magnetic condition. On the other hand, the voltage oscillogram is identical with the current oscillogram, except for drop of peak voltage.

In order to identify the roles played by external longitudinal magnetic field during the process of droplet transfer, some experiments are carried out using the high-speed camera. The transient behavior of droplet formation and transfer with different B are shown in the numbered images in Fig. 11. As demonstrated in Fig. 11a–b, whose B is 8 and 12 mT, it is obviously that the droplet direction parallel with the filler wire under 8 and 12 mT. The size of droplet is visibly smaller than that without magnetic field. With B increasing to 16 mT, the droplet does not form in the telos of filler wire but a bevel develops at the tip of wire,

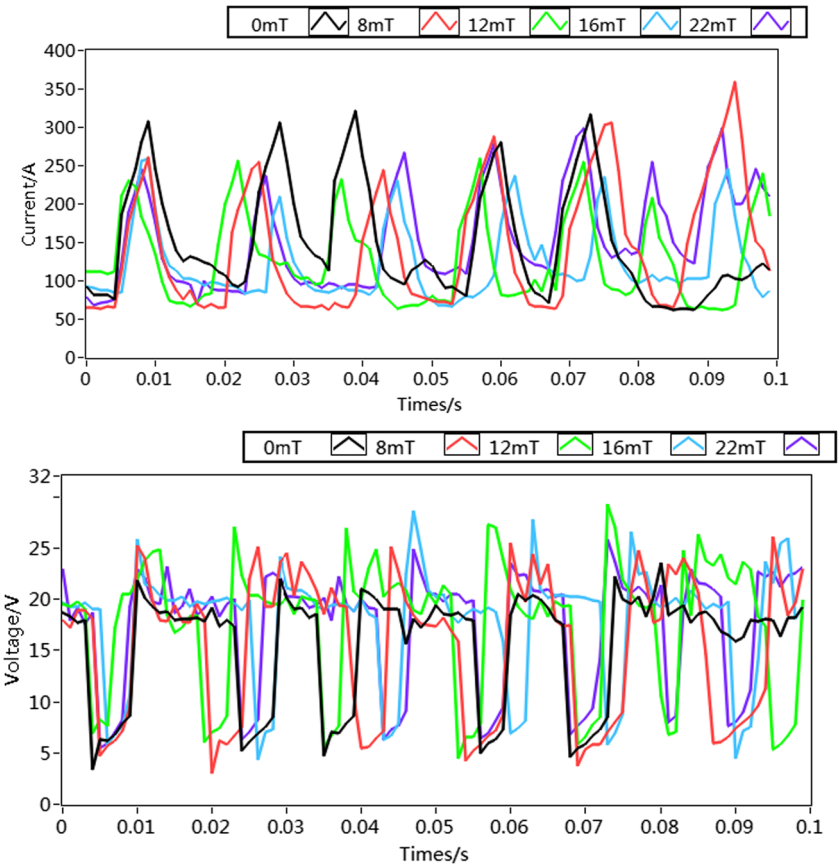

Fig. 10 Characteristics of current and voltage during hybrid welding for different magnetic induction intensity

where the droplet forms. In case of B increasing to 22 mT, this phenomenon is still observed. And the droplet forming in the bevel has a tendency to far away from filler wire telos.

Figure 12 displays impact of B on average droplet diameter (D) and transfer cycle time (T_C). It definitely indicates that the average droplet diameter decreases with B increasing. And when

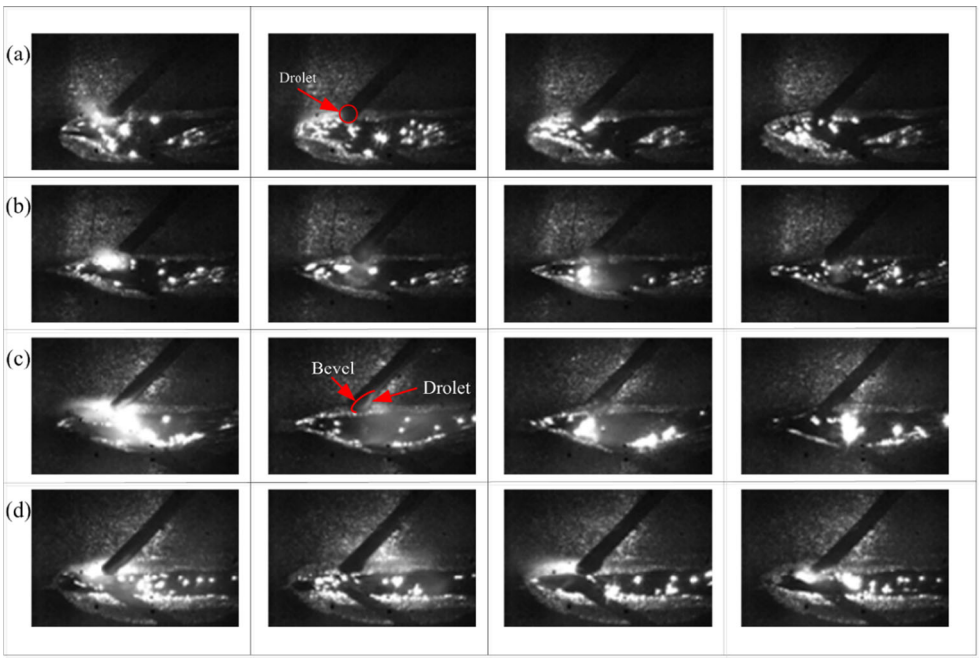

a: 8mT b: 12mT c: 16mT d: 22mT

Fig. 11 High-speed photographs of plasma with different magnetic induction intensity

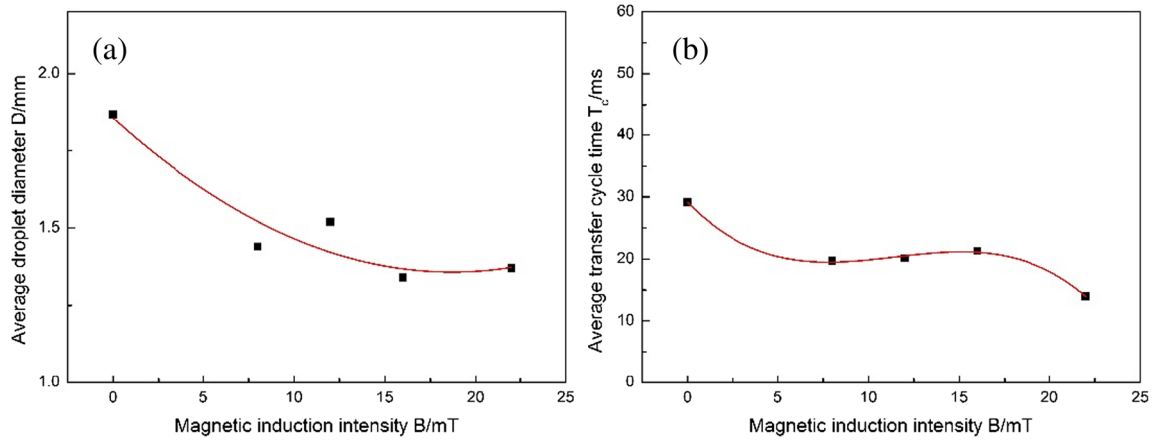

Fig. 12 Impact of magnetic induction intensity on average droplet diameter and transfer cycle time

B increases to 16 and 22 mT, the droplet diameter is almost invariability, which means the decrease of droplet diameter has a limitation. Furthermore, T_C with the magnetic field is lower than that without magnetic field. T_C is almost same when *B* strength is 8, 12, and 16 mT, and there is a decline of cycle time when *B* is 22 mT. For the short-circuiting transfer of laser-MIG hybrid welding, the smaller the droplet diameter and higher the frequency of short-circuiting, the closer the welding ripple and more stable of hybrid welding. Thus, the external magnetic field can improve the stabilization during hybrid welding process.

Results of part 3.2 mean that the droplet transfer under the magnetic field is greatly different from that without magnetic field on three aspects: direction of droplet changing, *D* and T_C decreasing. The droplet growing depends on heat of arc burning. When there is a magnetic field, T_C shortens which signifies that the time of arc burning shorten. Besides, magnetic field causes the decrease of arc root diameter. There two reason lead to the heat reducing of arc transmitting to the filler wire, making a decelerating of filler wire fusion velocity. Consequentially, the average droplet diameter will decrease. These two phenomenon is more remarkable with the increasing of magnetic induction intensity, so *D* decreases with the increasing of magnetic induction intensity.

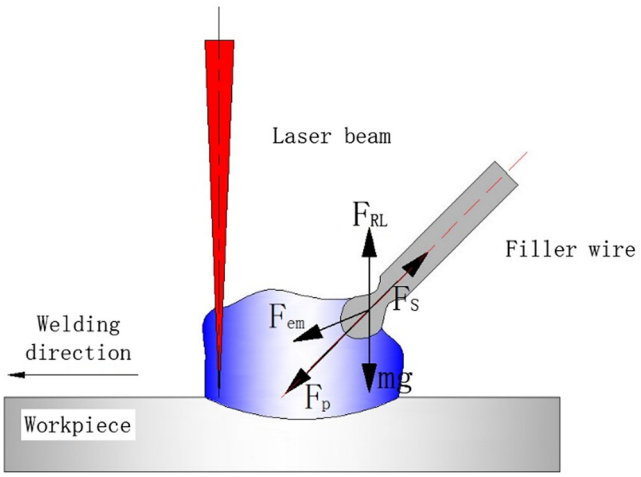

Fig. 13 Schematic of forces affecting droplet in hybrid welding

How the forces acting on the droplet determines the metal transfer process, such as droplet formation, direction, and cycle time. There are detaching forces and retention forces during hybrid welding process. As shown in Fig. 13, detaching forces include plasma drag force F_p, gravity force mg, electromagnetic force F_{em}, while retention forces include surface tension F_S and vapor jet force F_{RL}. As the results of part 3.1 show, the arc shape and direction of arc changed a lot, which has a significant effect on forces acting on the droplet. Combined with the high-speed images, the high-speed rotating arc makes the laser-induced plasma not eject upward directly, but eject along the rotating arc, causing the F_{RL} not acting on the droplet. Besides, owing to the change of the arc axis, F_p is changed along with the change of arc axis. Therefore, with *B* increasing, F_p is gradually far away from laser. These two reasons make the droplet direction changing with magnetic field.

Ulteriorly, this changing of arc can influence the current line distribution. The literature showed a close correlation between the current line distribution and the electromagnetic force F_{em}, which can be described by following Eq. [32]:

$$F_{em} = \frac{\mu_0 I^2}{4\pi}\left[\frac{2}{(1-\cos\theta)^2}\cdot\ln\left(\frac{1}{1+\cos\theta}\right)+\ln\left(\frac{r_d\sin\theta}{r_w}\right)-\frac{1}{1-\cos\theta}-\frac{1}{4}\right] \quad (1)$$

Where *I* is the welding current, r_d is the droplet radius, r_w is the wire radius, θ is the arc hanging angle and μ_0 is the permeability of free space. Figure 14 shows the current line distribution of different *B*. It is clear that θ is gradually decrease with *B* increasing, and the difficulty of a neck needing to be forming also reduces with *B* increasing because of the droplet diameter reducing. When there is not a magnetic field, part of the current lines go through the laser-induced plasma, making the rest of current lines leave the droplet from a smaller area at

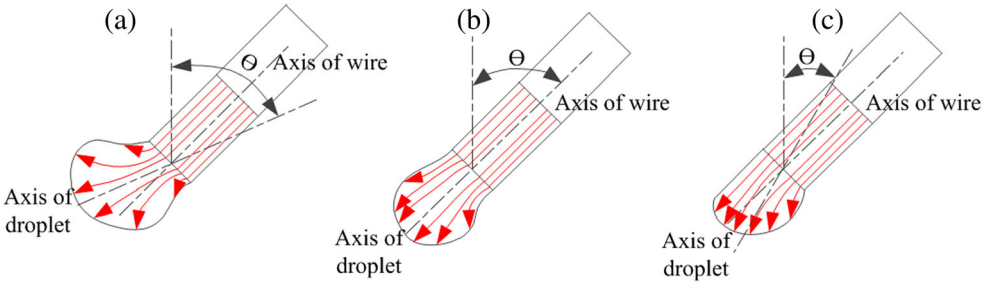

Fig. 14 Schemes of current lines' distributions with different magnetic induction intensity (*B*) **a** without magnetic field; **b** with relatively low magnetic induction intensity; **c** with relatively high magnetic induction intensity

the bottom of the droplet and thus induce an inward and upward electromagnetic force for repelling the droplet. With a relatively low *B*, as shown in Fig. 14b, current lines are more uniform and concentrated, and do not depend on the laser-induced plasma. Therefore, the direction of electromagnetic force is inward and downward for drive droplet. Following *B* increasing to relatively high, current lines is more concentrated than Fig. 14b, and the inward and downward electromagnetic force is more significant, which promotes the droplet transfer. Further, a group of electromagnetic force variation curves calculated with Eq. (1) for different *B* is shown in Fig. 15. Analysis indicates that F_{em} increases rapidly with *B* increasing. Thus, a neck will form and be broken faster with *B* increasing, making *Tc* shorter. On the other hand, the droplet diameter reducing and the peak current decreasing also prove that the droplet transfer is more easily and more smoothly. Consequentially, T_C becomes shorter assisted by external longitudinal magnetic field.

4 Conclusions

In this study, the effect of external longitudinal magnetic field on arc plasma characteristics and droplet transfer has been reported during laser-MIG hybrid welding. The results obtained in this research are summarized as follows:

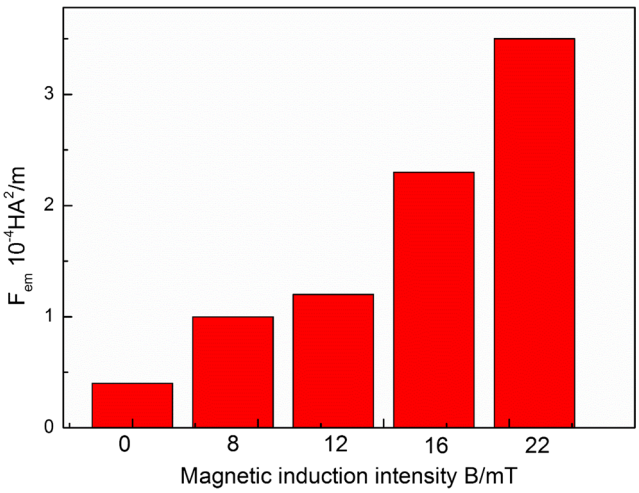

Fig. 15 Variation of electromagnetic force F_{em} with different magnetic induction intensity *B*

(1) The arc rotates and expands under an external longitudinal magnetic field, which makes the arc stiffness greatly enhances, and then the ability of arc resisting the laser-induced plasma attracting enhances. And the conductive path of arc changes from passing the laser-induced plasma to pass itself directly.
(2) The welding current and voltage waveforms indicate that the droplet transfer mode is short-circuiting transfer mode. With the magnetic induction intensity increasing in an appropriate range, the stableness of welding current and voltage enhances, and the peak current decreases compared with the situation of no magnetic field.
(3) The external longitudinal magnetic field significantly affects the forces acting on the droplet transfer. With the magnetic induction intensity increasing, the off-axis droplet gradually points to the axis of the filler wire. And when the magnetic induction intensity is relatively high, the end surface forms a bevel where droplet forms.
(4) As magnetic induction intensity increasing, because of current lines distributions, the electromagnetic force increasing, which results in the droplet diameter and transfer cycle time reducing obviously.

Acknowledgements This research effort was supported by the National Program on Key Basic Research Project (973 Program) of China (Grant No. 2014CB046703).

References

1. Steen WM (1980) Arc augmented laser processing of materials. J Appl Phys 51(13):5636–5641
2. Li ZY, Srivatsan TS, Li Y, Zhang WZ (2013) Coupling of laser with plasma arc to facilitate hybrid welding of metallic materials: a review. J Mater Eng Perform 22(2):384–395. doi:10.1007/s11665-012-0280-6
3. Zhang W, Hua XM, Liao W, Li F, Wang M (2014a) Behavior of the plasma characteristic and droplet transfer in CO2 laser-GMAW-P hybrid welding. Int J Adv Manuf Technol 72(5–8):935–942. doi:10.1007/s00170-014-5731-9
4. Wang J, Wang C, Meng X, Hu X, Yu Y, Yu S (2011) Interaction between laser-induced plasma/vapor and arc plasma during fiber laser-MIG hybrid welding. J Mech Sci Technol 25(6):1529–1533. doi:10.1007/s12206-011-0410-3
5. Gao M, Zeng X, Hu QW (2007) Effects of gas shielding parameters on weld penetration of CO2 laser-TIG hybrid welding. J Mater

Process Technol 184(1–3):177–183. doi:10.1016/j.jmatprotec.2006.11.019
6. Stute U, Kling R, Hermsdorf J (2007) Interaction between electrical arc and Nd: YAG laser-MIG hybrid welding. CIRP Ann 56(1):197–200
7. Campana G, Fortunato A, Ascari A, Tani G, Tomesani L (2007) The influence of arc transfer mode in hybrid laser-mig welding. J Mater Process Technol 191(1–3):111–113. doi:10.1016/j.jmatprotec.2007.03.001
8. Tani G, Campana G, Fortunato A, Ascari A (2007) The influence of shielding gas in hybrid LASER-MIG welding. Appl Surf Sci 253(19):8050–8053. doi:10.1016/j.apsusc.2007.02.144
9. Liu SY, Liu FD, Xu CY, Zhang H (2013) Experimental investigation on arc characteristic and droplet transfer in CO2 laser-metal arc gas (MAG) hybrid welding. Int J Heat Mass Transf 62:604–611. doi:10.1016/j.ijheatmasstransfer.2013.03.051
10. Zhang W, Hua XM, Liao W, Li F, Wang M (2014b) Study of metal transfer in CO2 laser+GMAW-P hybrid welding using argon-helium mixtures. Opt Laser Technol 56:158–166. doi:10.1016/j.optlastec.2013.08.006
11. Liu SY, Zhang H, Shi Y, Liu FD (2012a) Arc characteristic and behaviour of droplet transfer in CO2 laser-MAG hybrid welding of high strength steel. Laser Eng 23(1–2):29–42
12. Gao Z, Jiang P, Wang C, Shao X, Pang S, Zhou Q, Li X, Wang Y (2017) Study on droplet transfer and weld quality in laser-MIG hybrid welding of 316L stainless steel. Int J Adv Manuf Technol 88(1–4):483–493. doi:10.1007/s00170-016-8774-2
13. Le Guen E, Fabbro R, Carin M, Coste F, Le Masson P (2011) Analysis of hybrid Nd:Yag laser-MAG arc welding processes. Opt Laser Technol 43(7):1155–1166. doi:10.1016/j.optlastec.2011.03.002
14. Blinkov VA, Sheninkin MZ, Abralv MA (1975) Grains of solidifying metal refined under vibrations. Autom Weld 28(11):11–12
15. Luo J, Jia CS, Wang YS, Xue J, Wu YX (2001) Mechanism of the gas tungsten-arc welding in longitudinal magnetic field controlling. I. Property of the arc. Acta Metall Sin 37(2):212–216
16. Zhu S, Wang Q, Yin F, Liang Y, Wang X, Li X (2011) Research on MIG welding arc under alternating longitudinal magnetic field. Transactions of Materials and Heat Treatment 32(11):23–27
17. Chang YL, Liu MX, Lu L, Babkin AS, Lee BY (2015) The influence of longitudinal magnetic field on the CO2 arc shape. Plasma Sci Technol 17(4):321–326. doi:10.1088/1009-0630/17/4/11
18. Liu Y, Sun Q, Liu J, Wang S, Feng J (2015) Effect of axial external magnetic field on cold metal transfer welds of aluminum alloy and stainless steel. Mater Lett 152:29–31. doi:10.1016/j.matlet.2015.03.077
19. Luo J, Yao Z, Xue K (2016) Anti-gravity gradient unique arc behavior in the longitudinal electric magnetic field hybrid tungsten inert gas arc welding. Int J Adv Manuf Technol 84(1–4):647–661. doi:10.1007/s00170-015-7728-4
20. Hartz-Behrend K, Marqués JL, Forster G, Jenicek A, Müller M, Cramer H, Jilg A, Soyer H, Schein J (2014) Stud arc welding in a magnetic field—investigation of the influences on the arc motion. J Phys Conf Ser 550:012003. doi:10.1088/1742-6596/550/1/012003
21. Chang YL, Liu XL, Lu L, Babkin AS, Lee BY, Gao F (2014) Impacts of external longitudinal magnetic field on arc plasma and droplet during short-circuit GMAW. Int J Adv Manuf Technol 70(9–12):1543–1553. doi:10.1007/s00170-013-5403-1
22. Zhou J, Tsai H (2007) Application of Electromagnetic Force in Laser Welding. In: ASME 2007 International Mechanical Engineering Congress and Exposition, 2007. American Society of Mechanical Engineers, pp 1025–1030
23. Liu J, Hu W, Liu Y, Liu Y (2000) Analysis of the effect on electron density along the laser path by adding magnetic field in laser beam welding. In: Optics and Optoelectronic Inspection and Control: Techniques, Applications, and Instruments, 2000. International Society for Optics and Photonics, pp 236–239
24. Vollertsen F, Thomy C (2006) Magnetic stirring during laser welding of aluminum. J Laser Appl 18(1):28–34
25. Gatzen M, Tang Z, Vollertsen F, Mizutani M, Katayama S (2011) X-ray investigation of melt flow behavior under magnetic stirring regime in laser beam welding of aluminum. J Laser Appl 23(3):032002
26. Bachmann M, Avilov V, Gumenyuk A, Rethmeier M (2013) About the influence of a steady magnetic field on weld pool dynamics in partial penetration high power laser beam welding of thick aluminium parts. Int J Heat Mass Transf 60:309–321. doi:10.1016/j.ijheatmasstransfer.2013.01.015
27. Yu SF, Zhang YS, Lei Y, Xie ZQ, Wu DZ, Liu P (2006) The magnetic stirring mechanism of rotating magnetic field on non-magnetic alloy of laser welding. Transactions of the China Welding Institution 27(3):109–112
28. Bachmann M, Avilov V, Gumenyuk A, Rethmeier M (2014) Experimental and numerical investigation of an electromagnetic weld pool support system for high power laser beam welding of austenitic stainless steel. J Mater Process Technol 214(3):578–591
29. Sun Q, Wang J, Cai C, Li Q, Feng J (2016) Optimization of magnetic arc oscillation system by using double magnetic pole to TIG narrow gap welding. Int J Adv Manuf Technol 86(1–4):761–767. doi:10.1007/s00170-015-8214-8
30. Zhang X, Zhao Z, Wang C, Yan F, Hu X (2016) The effect of external longitudinal magnetic field on laser-MIG hybrid welding. Int J Adv Manuf Technol 85(5):1735–1743. doi:10.1007/s00170-015-8035-9
31. Hua AB, Yin SY, Chen SJ, Bai SJ, Zhang XL (2010) Behavior of arc and drop transfer of MAG welding controlled by longitudinal magnetic field. Chinese Journal of Mechanical Engineering 46(14):95–100
32. Liu S, Liu F, Zhang H, Shi Y (2012b) Analysis of droplet transfer mode and forming process of weld bead in CO 2 laser–MAG hybrid welding process. Opt Laser Technol 44(4):1019–1025